Journal of Bioscience and Bioengineering
VOL. 127 No. 2, 138–144, 2019

www.elsevier.com/locate/jbiosc

Biochemical characterization of isoprene synthase from *Ipomoea batatas*

Meijie Li,[1,2] Changqing Liu,[1,2] Hailin Chen,[1,2] Li Deng,[1] Haibo Zhang,[1] Rui Nian,[1] and Mo Xian[1,*]

Key Laboratory of Biobased Materials, Qingdao Institute of Bioenergy and Bioprocess Technology, Chinese Academy of Sciences, Qingdao 266101, PR China[1] *and University of Chinese Academy of Sciences, Beijing 100049, PR China*[2]

Received 18 March 2018; accepted 24 July 2018
Available online 3 September 2018

The bio-production process of isoprene, an essential chemical used in industry, is strongly limited by isoprene synthase. In our previous work, relatively high isoprene production was observed with isoprene synthase from *Ipomoea batatas* ($IspS_{ib}$). In this work the biochemical properties of $IspS_{ib}$ were analyzed and compared with those of isoprene synthase from *Populus alba* ($IspS_{pa}$) and other species. Firstly, $IspS_{ib}$ and $IspS_{pa}$ were expressed, purified, and identified by SDS-PAGE and western blot analysis. Secondly, pH and temperature dependence of $IspS_{ib}$ were performed and an optimum pH of 8.6 and an optimum temperature of 42 °C were resulted. Mg^{2+} with optimum concentration of 56 mM was proved to be needed for enzyme activation. In addition, *in vivo* and *in vitro* study of the thermostabilities of $IspS_{ib}$ and $IspS_{pa}$ were performed. The enzyme activity of $IspS_{ib}$ and $IspS_{pa}$ dropped very rapidly after incubation at 30 °C; almost 80% enzyme activity of $IspS_{ib}$ was lost after 20 min of incubation. Moreover, the Michaelis–Menten constant was measured. $IspS_{ib}$ showed a lower K_m, 0.2 mM, and a higher k_{cat}, 0.37 s^{-1}, as compared with $IspS_{pa}$. The high catalytic efficiency, which was reflected by the high k_{cat}/K_m ratio, indicates that $IspS_{ib}$ is a good candidate for the bio-isoprene production, while its thermal instability remains as a challenge. Enzyme engineering efforts, such as direction evolution or semi-rational evolution, are planned for further research.

[**Key words:** Isoprene synthase; *Ipomoea batatas*; Characterization; Thermostability; Enzyme]

Plants have been reported to emit isoprene, which process shows a protective effect against environment stresses such as high temperature, reactive oxygen (1), drought (2), and herbivory (3). In industry, isoprene is a platform chemical that is used for the production of rubber, pesticides, medicines, oil additives, fragrances, and biofuels (4,5). Annually, 800,000 tons of isoprene monomer are produced by petroleum cracking, a procedure that is environmentally damaging and produces unrecyclable materials (6). In the last fifteen years, because of the oil crisis and environment stress, researchers have focused on the microbial production of isoprene. Isoprene is synthesized from dimethylallyl diphosphate (DMAPP) through catalysis of isoprene synthase (IspS). The synthesis of DAMPP proceeds through the methylerythritol phosphate pathway or the mevalonate (MVA) pathway (7).

IspS was demonstrated to be the rate-limiting enzyme and our understanding of IspS is limited. In plants, IspSs have been found to be located in the chloroplast and isoprene production is regulated by the expression and activity of IspS and the pool size of DMAPP (8–10). No IspS has been found in microorganisms, although isoprene production has been detected in *Bacillus subtilis* (11). Several genes encoding IspS from plant species have been cloned and analyzed, such as those of *Populus alba*, *Populus* × *canescens*, and *Pueraria montana* (12–14). However, IspSs from different species show similar enzymatic properties. All analyzed IspSs have very high K_m values, in the millimolar range, for the substrate DMAPP, in contrast to other terpene synthases, which have K_m values in the micromolar range (15). The crystal structure of IspS from a gray poplar hybrid shows two unique Phe residues (F338 and F485 in IspS from *P. alba*) which was speculated to be critical to reducing the size of the substrate (DMAPP) binding site, leading to high K_m values (16,17). The k_{cat} values of known IspSs are relatively low, in the range of 0.011–1.7 s^{-1} (18). Therefore, screening of enzymes with high k_{cat} and low K_m value is still the main barrier for bio-isoprene production.

IspSs from *P. alba* ($IspS_{pa}$) and *P. montana* ($IspS_{pm}$) are commonly used because they usually lead to high level isoprene production (6,19). Enzyme activity assays have shown that $IspS_{pa}$ and $IspS_{pm}$ have high K_m and low k_{cat} values (12,14,18,20). The strain modified with IspS from *Ipomoea batatas* ($IspS_{ib}$) accumulates two-fold the amount of isoprene of the strain with $IspS_{pa}$ (16). This finding indicates that $IspS_{ib}$ may have better enzyme activity than the widely used IspSs. Moreover, the well-characterized IspSs mainly come from plants belong to the class of Archichlamydeae, while *I. batatas* belong to Sympetalae, another division of Dicotyledoneae, in which IspSs have not been characterized. The data of plant classification was obtained from iplant (http://bk.iplant.cn).

In this study, the biochemical characterization of $IspS_{ib}$ was reported and compared with $IspS_{pa}$ and IspSs from other species. $IspS_{ib}$ was heterogeneously expressed in *Escherichia coli* and

* Corresponding author at: Qingdao Institute of Bioenergy and Bioprocess Technology, Chinese Academy of Sciences, No. 135 Songling Road, Qingdao 266101, PR China. Tel.: +86 0532 80662768; fax: +86 0532 80662765.

E-mail addresses: li_mj@qibebt.ac.cn (M. Li), liucq@qibebt.ac.cn (C. Liu), chenhl@qibebt.ac.cn (H. Chen), dengli@qibebt.ac.cn (L. Deng), zhanghb@qibebt.ac.cn (H. Zhang), nianrui@qibebt.ac.cn (R. Nian), xianmo1@qibebt.ac.cn (M. Xian).

1389-1723/$ – see front matter
https://doi.org/10.1016/j.jbiosc.2018.07.022

purified. Biochemical characteristics such as pH dependence, temperature dependence, metal-ion preference, thermostability, K_m, and k_{cat} were measured. We also summarize the enzyme parameters of IspSs from different species.

MATERIALS AND METHODS

Strains and plasmids All strains, plasmids and primers used in this study are listed in Table 1. $IspS_{ib}$ and $IspS_{pa}$ were separately cloned into pACYCDuet-1 plasmid (Novagen, Germany). Polymerase chain reaction (PCR) was performed for sequence amplification by 2 × PCR Bestaq MasterMix (Applied Biological Materials Inc., Richmond, BC, Canada) with the primers (synthesized by Genewiz, Suzhou, PR China), $IspS_{ib}$-F/R and $IspS_{pa}$-F/R (Table 1). Plasmid pACYCDuet-1 was digested by restriction enzymes, *Nde*I and *Bgl*II (Thermo Scientific, Waltham, MA, USA). A ligation-free cloning system (Applied Biological Materials Inc.) was utilized for sequence ligation. The constructed plasmids, pACYC-$IspS_{ib}$ and pACYC-$IspS_{pa}$, were separately transformed into *E. coli* Bl21(DE3) to build the strains LMJ-ib and LMJ-pa (Table 1).

$IspS_{ib}$ and $IspS_{pa}$ expression and purification The expression and purification process were performed as described by Sharkey et al. (12) with some modification. *E. coli* strains were grown in LB medium. For $IspS_{ib}$ and $IspS_{pa}$ expression, recombinant strains were cultured in shake-flask fermentation with LB medium. Seed cultures were obtained and transferred into 100 mL LB medium added with appropriate antibiotics (34 μg mL^{-1} of Chloramphenicol), cultured at 37 °C, and induced with 0.5 mM isopropyl-β-D-thiogalactoside (IPTG) solution at OD600 0.6–0.8. Further cultivation was performed at 30°C for 6 h. Cells were collected by centrifugation at 5000 × *g* for 15 min. The cell pellet was resuspended in cell lysis buffer (Beyotime, Shanghai, PR China) and then stored on ice for 1 h. Centrifugation at 5000 × *g* for 30 min was conducted to separate the soluble protein and other cell fragments. The protein-containing supernatant was harvested and passed through a BeyoGold His-tag purification resin (Beyotime). The imidazole was removed using an Amicon Ultra-15 centrifugal filter units (Millipore, Billerica, MA, USA). The unpurified and purified proteins were confirmed by SDS-PAGE and western blot analysis. A BCA protein assay kit (Beyotime) was used to determine the concentration of the purified protein, which was used for further enzyme assay.

IspS enzyme assay IspS activity was assayed in a 100 μL reaction mixture containing 50 mM HEPES buffer (pH 7.8), 50 mM KCl, 50 mM $MgCl_2$, 5 μL of glycerol (Sinopharm, Shanghai, PR China), 5 mM DTT (Beyotime), 1 mM DMAPP (Cayman Chemical, Ann Arbor, MI, USA), and 1 μg of purified enzyme, as described by Gao et al. (21). The reaction was carried out in a 2 mL glass vial, which was immediately sealed with a rubber lid after the enzyme was added. The reaction mix was incubated at 37°C for 10 min, and 500 μL of gas in the headspace was sampled for gas chromatography detection. Gas chromatography detection of isoprene was performed as previously described (22).

For the pH dependence assay, buffers (50 mM) with different pH values were used: citrate buffer (pH 3, 5, and 6), HEPES buffer (pH 6.8 and 7.8), glycine-NaOH buffer (pH 8.6, 9.2, 9.8, and 10.6), and NaOH solution (pH 12). Temperature profiling was performed by incubating the reactions at temperatures ranging from 20°C to 55°C. The enzyme activity in the reaction system with different divalent cations (Mg^{2+}, Mn^{2+}, Fe^{2+}, Co^{2+}, Cu^{2+}, Zn^{2+}, Ni^{2+}, and Ca^{2+}) was also assayed, and ethylene diamine tetraacetic acid (EDTA) was used as control. The optimum concentration of the divalent cation Mg^{2+} for enzyme activity was then assayed from 1 mM to 500 mM. Gaussian fitting method was carried out to predict the optimum pH, temperature, and Mg^{2+} concentration. The substrate dependence of IspS was studied by adding DMAPP with different concentrations to the reaction mixtures: 0 μM, 25 μM, 50 μM, 0.1 mM, 0.2 mM, 0.3 mM, 0.4 mM, 0.5 mM, 0.6 mM, 0.8 mM, 1 mM, 4 mM, 8 mM, and 15 mM. Lineweaver–Burk plot analysis was applied to estimate K_m, V_{max}, and k_{cat} values. SciDAVis program was used for data analyzing.

Thermostabilities of $IspS_{ib}$ and $IspS_{pa}$ The purified $IspS_{ib}$ and $IspS_{pa}$ were incubated at 30°C, 40°C, and 50°C and then sampled at 10 min, 20 min, 40 min, and 60 min. The enzyme was placed on ice immediately, and enzyme activity assay was performed as described above. Moreover, the purified $IspS_{ib}$ enzyme was incubated at 4°C, 16°C, 37°C, 42°C, and 55°C, separately, and sampled at 2 h, 4 h, 8 h, 1 day, 2 days, 3 days, 4 days, 5 days, and 6 days for SDS-PAGE analysis. To test the $IspS_{ib}$ stability *in vivo*, strain LMJ11, described in Table 1, was cultured as mentioned above. The cells were collected at different times after induction. SDS-PAGE analysis was conducted to detect protein accumulation during fermentation.

RESULTS AND DISCUSSION

In our previous study, $IspS_{ib}$ was introduced into *E. coli* Bl21(DE3) with the entire MVA pathway (unpublished data). The engineered strain, LMJ11, had higher isoprene production than the strain in which $IspS_{pa}$ is utilized. To learn more about $IspS_{ib}$, biochemical characterization of $IspS_{ib}$ was performed in this study, especially the enzyme stability, which has not been researched previously. This is the first time that IspS from Sympetalae, a division of the class Dicotyledoneae, is assayed.

Heterogeneous expression and purification of $IspS_{ib}$ and $IspS_{pa}$ Plasmids pACYC-$IspS_{ib}$ were constructed and transformed into *E. coli* Bl21(DE3). The engineered strain was cultured and $IspS_{ib}$ was expressed. SDS-PAGE analysis revealed that soluble $IspS_{ib}$ protein (63 kDa) was successfully expressed (Fig. 1A). Afterward, purification of $IspS_{ib}$ was conducted and SDS-PAGE and western blot assay showed that $IspS_{ib}$ was successfully purified (Fig. 1A). Similarly, pACYC-$IspS_{pa}$ was constructed and $IspS_{pa}$ was expressed and purified successfully (Fig. 1B). The biochemical activity of the purified $IspS_{ib}$ was assayed and compared with $IspS_{pa}$.

Effect of pH and temperature on the activity of $IspS_{ib}$ The enzyme assay of $IspS_{ib}$ within a large pH range (pH 3–12) was performed using different buffer systems. A typical Gaussian distribution curve, also called a bell-shaped curve, was obtained (Fig. 2). The highest enzyme activity was observed at pH 8.5. Gaussian fitting method showed that the optimum pH of $IspS_{ib}$ is 8.6, similar to IspSs from *Campylopus introflexus* and *Quercus petraea* (Table 2) (23,24). The optimum pH values of IspSs from several plant species were summarized and the data indicate that IspSs show high enzyme activity in the alkaline buffer solution (Table 2).

The enzyme activity of $IspS_{ib}$ under different temperature was also explored. The enzymatic reactions were performed at different temperatures (20°C–50°C). Highest isoprene production was detected at 42°C, and a bell-shaped curve was also obtained (Fig. 3). Gaussian fitting method showed that the optimum temperature of

TABLE 1. Plasmids, strains, and primers in this study.

Plasmid/Strain/Prime	Description	Reference
Plasmid		
pACYC-$IspS_{ib}$	pACYCDuet-1 carrying $IspS_{ib}$ from *I. batatas*	This study
pACYC-$IspS_{pa}$	pACYCDuet-1 carrying $IspS_{pa}$ from *P. alba*	This study
pYJM14	pTrcHis2B carrying ERG12, ERG8, ERG19 and IDI1 from *Saccharomyces cerevisiae*	22
pA-MM-$ispS_{ib}$	pACYCDuet-1 carrying mvaE and mvaS from *Enterococcus faecalis*, and $IspS_{ib}$ from *I. batatas*	Unpublished data
Strain		
LMJ-ib	Bl21(DE3)/pACYC-$IspS_{ib}$	This study
LMJ-pa	Bl21(DE3)/pACYC-$IspS_{pa}$	This study
LMJ11	Bl21(DE3)/pYJM14 + pA-MM-$ispS_{ib}$	Unpublished data
Primer		
$IspS_{ib}$-F	GGAGATATACATATGAGTAGCGCCCAGAATC	This study
$IspS_{ib}$-R	ATCCAATTGAGATCTATGATGATGATGATGATGTGCTTCAACCGGATT	This study
$IspS_{pa}$-F	GGAGATATACATATGAGATGTAGCG	This study
$IspS_{pa}$-R	ATCCAATTGAGATCTTTAATGATGATGATGATGATGTGCGCGTTCAAACGGCAGAA	This study

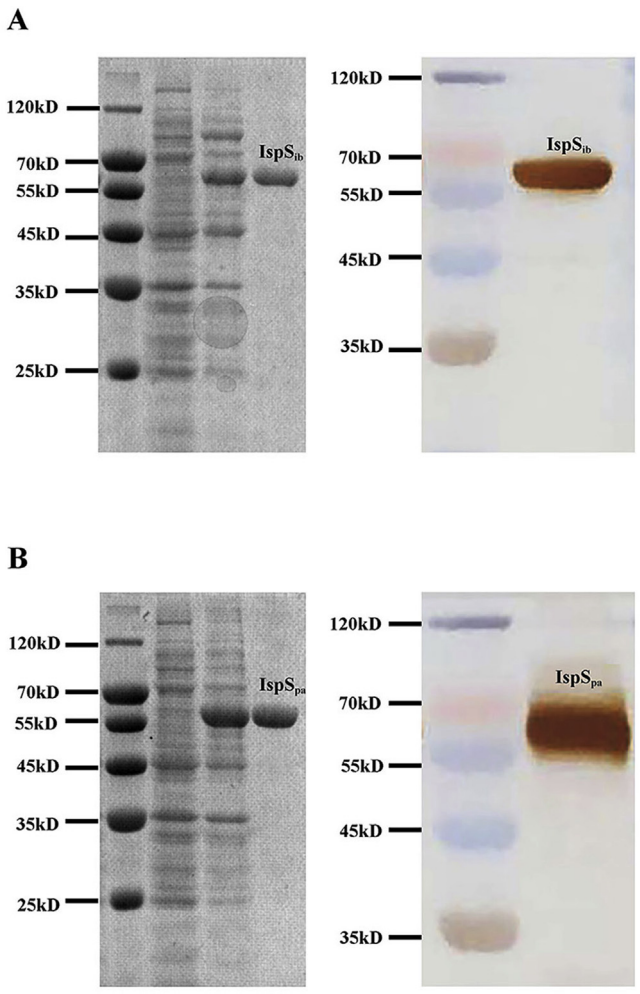

FIG. 1. Recombinant expression and purification of IspS$_{ib}$ and IspS$_{pa}$. (A) SDS-PAGE analysis and western-blot analysis results for the expressed and purified IspS$_{ib}$ (63 kDa). (B) SDS-PAGE analysis and western-blot analysis results for the expressed and purified IspS$_{pa}$ (64 kDa).

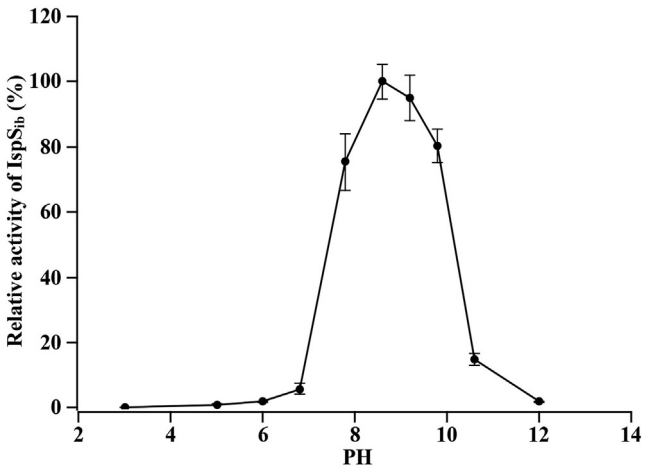

FIG. 2. pH dependence of IspS$_{ib}$ activity. Reaction mixtures containing 1 μg of purified enzyme, 1 mM DMAPP, 5 % glycerol, 5 mM DTT, 50 mM $MgCl_2$, and 50 mM KCl were incubated with buffers with pH ranging from 3 to 12, at 37°C. Values are reported as mean ± SD of triplicate experiments.

IspS$_{ib}$ was 42°C, similar to most of the IspSs from other organisms, including *Populus* × *canescens* and *P. montana* (13,18). The optimum temperatures of IspSs from different plant species were summarized and the data show that most IspSs have high enzyme activity at 40–45°C, except for the IspSs from the genus *Quercus*, with high enzyme activity at 35°C or 50°C (Table 2). However, the enzyme activity of IspS$_{ib}$ dropped rapidly between 42°C and 55°C and a right-skewed distribution plot was observed (Fig. 3). The similar rapid decline of enzyme activity at high temperature were also observed in IspSs from other organisms (20,23,25,26).

For fermentation, the engineered strain was usually cultivated at 30°C, and the pH value was maintained at 7 (22). However, the optimum pH and temperature of IspSs, summarized in Table 2, are far from the culture conditions. For IspS$_{ib}$, greatly declined enzyme activity, 19% at 30°C and 11% at pH 7, were detected (Figs. 2 and 3). We can therefore reasonably speculate that the inappropriate culture conditions during the fermentation of the engineered strain contributes to the low-level isoprene production. IspSs, including IspS$_{ib}$, require further enzyme engineering to show high enzyme activity under normal culture conditions (30°C and pH 7), which thus improves isoprene production.

Metal-ion dependence of IspS$_{ib}$ The effect of metal ions, mostly divalent cations, on the catalytic activity of the IspS$_{ib}$ was examined. The highest isoprene production in the presence of Mg^{2+} was measured (Fig. 4A). Considering the enzyme activity in the presence of Mg^{2+} as 100%, we measured the activities in the presence of Mn^{2+}, Fe^{2+}, Co^{2+}, Cu^{2+}, Zn^{2+}, and Ni^{2+}. Declined enzyme activity, 28%, 6%, 6%, 6%, 4%, and 1% were resulted (Fig. 4A). No enzyme activity was detected in the presence of Ca^{2+} or EDTA (Fig. 4A). The preferences for divalent cations of IspSs from various species were summarized. The data show that Mg^{2+} or Mn^{2+} is required for IspSs enzyme activity (Table 2). Since IspS$_{ib}$ showed preference for Mg^{2+}, we measured optimum Mg^{2+} concentration for enzyme activation. When the Mg^{2+} concentration was less than 50 mM, the enzyme activity improved rapidly along with the increase in Mg^{2+} concentration, resulting in a steep slope (Fig. 4B). When the Mg^{2+} concentration was more than 50 mM, however, a gradual decline in specific activity was detected (Fig. 4B). Gaussian fitting method showed that the optimum Mg^{2+} concentration is 56 mM. Similar sharp increase and gradual decrease of enzyme activity with different metal ion (Mn^{2+}) concentration was observed for IspS from *Casuarina equisetifolia* (20). However, for IspS from *C. intraflexus*, no decrease of enzyme activity with increasing metal ion (Mn^{2+}) concentration was observed (23). We think further study is needed to decipher the decreased enzyme activity with high metal ion concentration.

Thermal instability of IspS$_{ib}$ Aside from the enzyme parameters mentioned above, the stability of IspS$_{ib}$ was also determined in this study. Shake-flask fermentation of strain LMJ11, with IspS$_{ib}$ and the entire MVA pathway genes expressed, was performed. The protein expression levels were monitored by SDS-PAGE analyses at different times after induction (Fig. 5A). The accumulated IspS$_{ib}$ increased along with the induction time and a clear IspS$_{ib}$ band appeared at 7 h after induction (Fig. 5A). The decreased accumulation of IspS$_{ib}$ at 21 h after induction was observed, which was indicated by the weakened IspS$_{ib}$ band (Fig. 5A). However, the accumulation of other enzymes, MvaE, ERG8/ERG12, ERG19 and MvaS, in the heterogeneous MVA pathway remained stable at 21 h after induction (Fig. 5A). In a previous study, IspS$_{pm}$ showed declined accumulation at 40 h after induction, later than the decrease of IspS$_{ib}$ (18). Isoprene productivity at different time after induction was also measured (data not shown). Interestingly, the data indicate that isoprene production is correlated with the level of accumulated IspS$_{ib}$. In conclusion, the SDS-PAGE analysis indicated

TABLE 2. Comparison of biochemical characteristics of IspSs.

IspS Source	K_m^{DMAPP} (mM)	k_{cat} (s^{-1})	pH	Temperature (°C)	Cofactors	References
Ipomoea batatas	0.2	0.37	8.6	42	Mg^{2+}	This study
Eucalyptus globulus	0.2	0.195	N/A	N/A	N/A	28
Casuarina equisetifolia	0.3	0.015	8.0	40	Mn^{2+}	20
Campylopus introflexus	0.37 ± 0.28	N/A	8.6 ± 0.5	40 ± 3	Mn^{2+}	23
Quercus rubur L.	0.53	N/A	7.3–7.7	50	N/A	25
Quercus petraea	0.97	N/A	8.5	35	Mg^{2+} >Mn^{2+}>Zn^{2+}	24
Populus × *canescens*	2.45±0.1	N/A	7.0–8.5	40	Mg^{2+}	13
Pueraria montana	7.7	0.088	N/A	N/A	N/A	12
	2.5	4.4	7.5	42	Mg^{2+}	18
Ficus septica	3.4	0.011	9.5	40	Mg^{2+}	20
Populus tremuloides	8	1.7	8	N/A	Mg^{2+} or Mn^{2+}	29,30
Populus alba	8.7	0.03	8	40	Mg^{2+}	14
	15.9	0.034	N/A	45	Mg^{2+}	20
	0.34	0.15	N/A	N/A	N/A	This study
Salix discolor L. (thylakoid-bound)	8	N/A	10	N/A	Mg^{2+}/Mn^{2+}	31
Salix discolor L. (stromal)	1–8	N/A	8	N/A	Mg^{2+}	32
Mucuna sp.	9	N/A	7.8–8.5	N/A	Mg^{2+} >Mn^{2+}	33
Bacillus subtilis	N/A	N/A	6.2	N/A	Mg^{2+}/Mn^{2+}	11
Ficus virgata	N/A	N/A	10.0	40	Mg^{2+}	20

that decreased accumulation of $IspS_{ib}$ appeared at 21 h after induction, earlier than other over-expressed enzymes.

The stability of $IspS_{ib}$ was also estimated *in vitro*. SDS-PAGE was performed to analyze $IspS_{ib}$ after exposure to different heat conditions. When $IspS_{ib}$ was incubated at 4°C, almost no degradation was detected after 6 days (Fig. 5B). Degradation of $IspS_{ib}$ was observed after incubation at 16°C for 2 days (Fig. 5B). After 8 h of incubation at 37°C and 42°C, part of the $IspS_{ib}$ was degraded and no $IspS_{ib}$ was detected after 6 days (Fig. 5B). Rapid $IspS_{ib}$ degradation was observed after incubation at 55°C, and virtually no $IspS_{ib}$ was detected after 3 days (Fig. 5B). Moreover, $IspS_{ib}$ was exposed to different temperatures for different durations, and the enzyme activity was measured afterward. Considering the enzyme activity of $IspS_{ib}$ before heat exposure as 100%, we measured the relative enzyme activity after incubation at different heating temperatures. The data indicated that after incubation at 30°C for 10 min, only 62% of the enzyme activity remained. Only 8% of the enzyme activity remained after 60 min of incubation at 30°C (Fig. 5C). After 10 min of incubation at 40°C, most of the enzyme activity (84%) was lost (Fig. 5C). Almost no enzyme activity remained after 40 min of incubation at 40°C (Fig. 5C). When the enzyme was incubated at 50°C or 60°C, no enzyme activity was detected after 10 min (Fig. 5C). These results indicate that $IspS_{ib}$ was deactivated rapidly. Similarly, the enzyme activity of $IspS_{pa}$ was also measured after different incubation times at 30°C, 40°C, and 50°C. The results indicated that $IspS_{pa}$ lost its enzyme activity quickly, but not as fast as $IspS_{ib}$ did (Fig. 5C). Combining the enzyme activity data and SDS-PAGE data, we found that loss of enzyme activity of $IspS_{ib}$ was rapid during heat incubation; however, the degradation rate of the enzyme was relatively low.

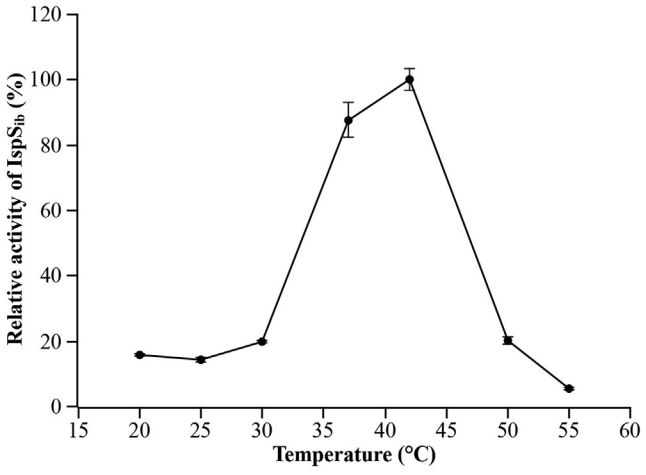

FIG. 3. Temperature dependence of $IspS_{ib}$ activity. IspS activity was assayed in 50 mM HEPES buffer (pH 7.8) containing 50 mM KCl, 50 mM $MgCl_2$, 5 μL of glycerol, 5 mM DTT, 1 mM DMAPP, and 1 μg of purified enzyme at temperatures ranging from 20°C to 55°C. Values are reported as mean ± SD of triplicate experiments.

For the first time, the enzyme activity of $IspS_{ib}$ and $IspS_{pa}$ at different temperatures and at different incubation times were measured. IspSs from other species have not been studied for the same property. During fermentation, $IspS_{ib}$ was mostly accumulated at 7 h–15 h after induction, and decrease was observed after 21 h. Considering the rapid loss of enzyme activity and low speed degradation, we reasonably speculate that during fermentation, most of the accumulated $IspS_{ib}$ during 7 h–15 h after induction was inactive. $IspS_{ib}$ is a thermally unstable enzyme and that further study of its structure is necessary. The instability of $IspS_{ib}$ may be relevant to the $IspS_{ib}$ expression and the functions of isoprene in the plant. Isoprene is produced and emitted into the air under stressful conditions, such as high temperature and drought (2), as discussed in the introduction section. IspS activity and expression also displays diurnal variation, high during light and low under dark (27). This property suggests that IspS is not a constitutive expression enzyme and that the expression and degradation are tightly regulated by the whole system. In conclusion, $IspS_{ib}$ is a thermal unstable enzyme and this instability maybe related to the intermittent $IspS_{ib}$ expression in plant.

Kinetic parameters of $IspS_{ib}$ The dependence of $IspS_{ib}$ on DMAPP concentration was measured. When the concentration of DMAPP was below 0.6 mM, the isoprene productivity increased along with the increase in DMAPP concentration. However, higher DMAPP concentrations (>0.6 mM) inhibited enzyme activity (Fig. 6A). The similar isoprene production (between 20 and 40 nmol mg^{-1} min^{-1}) resulted when the DMAPP concentration ranged from 4 mM to 15 mM. Lineweaver–Burk plot analysis was performed to estimate K_m and V_{max}, choosing the data for DMAPP concentrations of 0 mM–0.6 mM (Fig. 6B). The apparent K_m of $IspS_{ib}$ was 0.2 mM, and the V_{max} was 0.36 μmol (mg protein)$^{-1}$ min^{-1}, while k_{cat} was 0.37 s^{-1}. The k_{cat}/K_m ratio of $IspS_{ib}$ was determined to be 1.85. The K_m and k_{cat} values of $IspS_{pa}$ were measured for comparison. Unlike in the case of $IspS_{ib}$, no reduction of enzyme activity at high substrate DMAPP concentration was observed (Fig. 6C). Higher K_m (0.34 mM) and lower k_{cat} (0.15 s^{-1}) values as compared with those of IspSib were obtained. The k_{cat}/

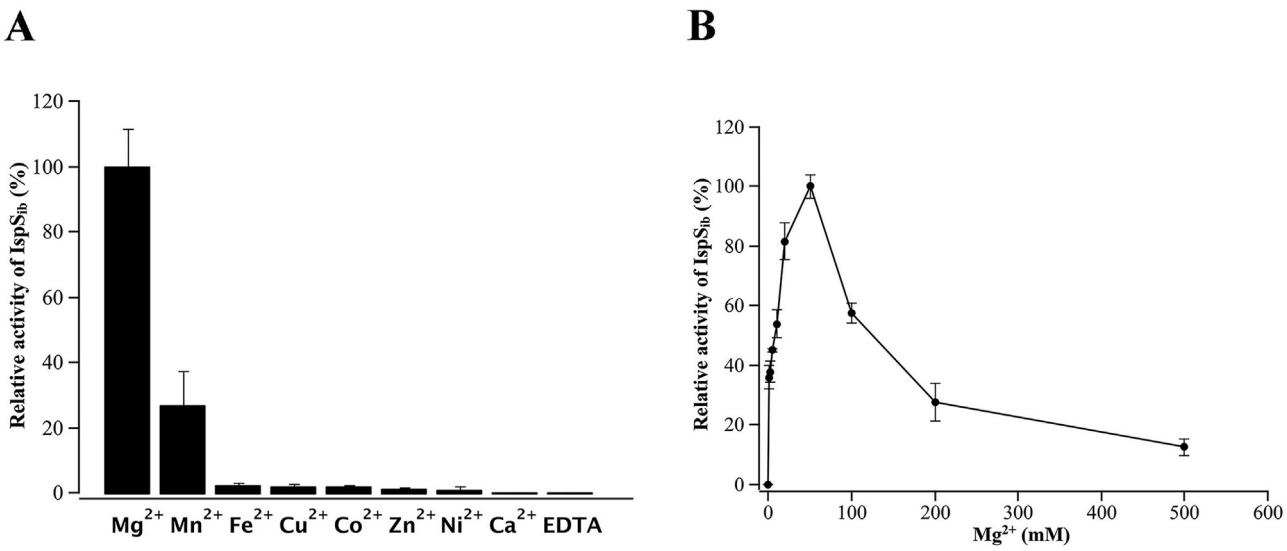

FIG. 4. Divalent cation requirement of the $IspS_{ib}$ activity. (A) Reaction mixtures containing 1 μg of purified enzyme, 1 mM DMAPP, 5 % glycerol, 5 mM DTT, and 50 mM KCl in 50 mM HEPES buffer (pH 7.8), as well as several kinds of added divalent cations, were incubated at 37°C. (B) Mg^{2+} at different concentrations was added to the reaction mixtures described above. Values are reported as mean ± SD of triplicate experiments.

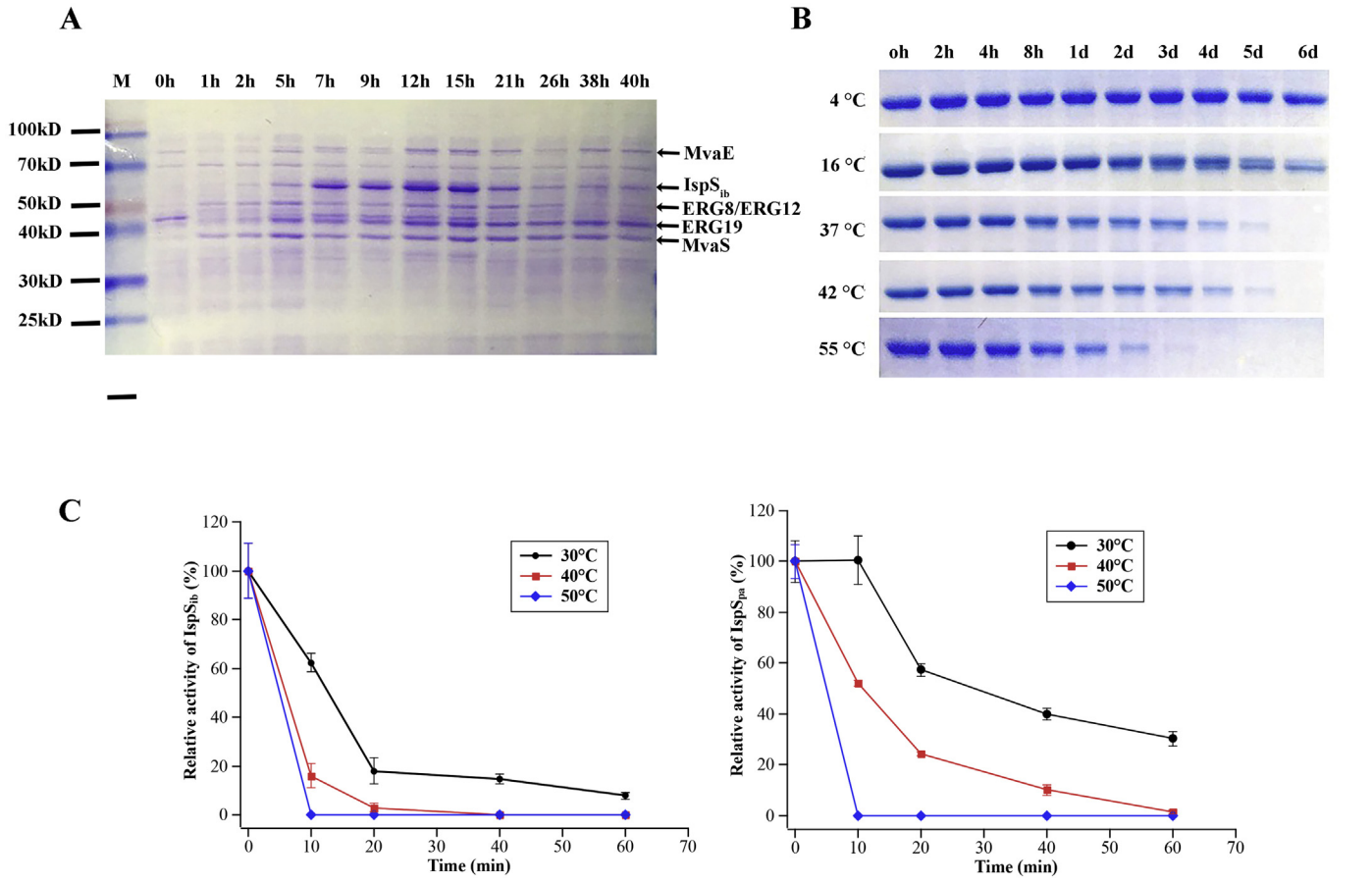

FIG. 5. Thermostabilities of $IspS_{ib}$ and $IspS_{pa}$. (A) The stability of $IspS_{ib}$ *in vivo*, as evaluated through the accumulation of enzyme after induction. M: molecular weight marker; 0 h–40 h: number of hours after induction. Bands for different enzymes were labeled. (B) The degradation of $IspS_{ib}$ *in vitro*, as indicated by SDS-PAGE analysis after exposure to different temperatures (4°C, 16°C, 37°C, 42°C, and 55°C) for 2 h, 4 h, 8 h, 1 day, and 6 days. (C) Thermostabilities of $IspS_{ib}$ and $IspS_{pa}$ as evaluated by measurements of enzyme activity after exposure at 30°C, 40°C, and 95°C for 10 min, 20 min, 40 min, and 60 min. Values are reported as mean ± SD of triplicate experiments.

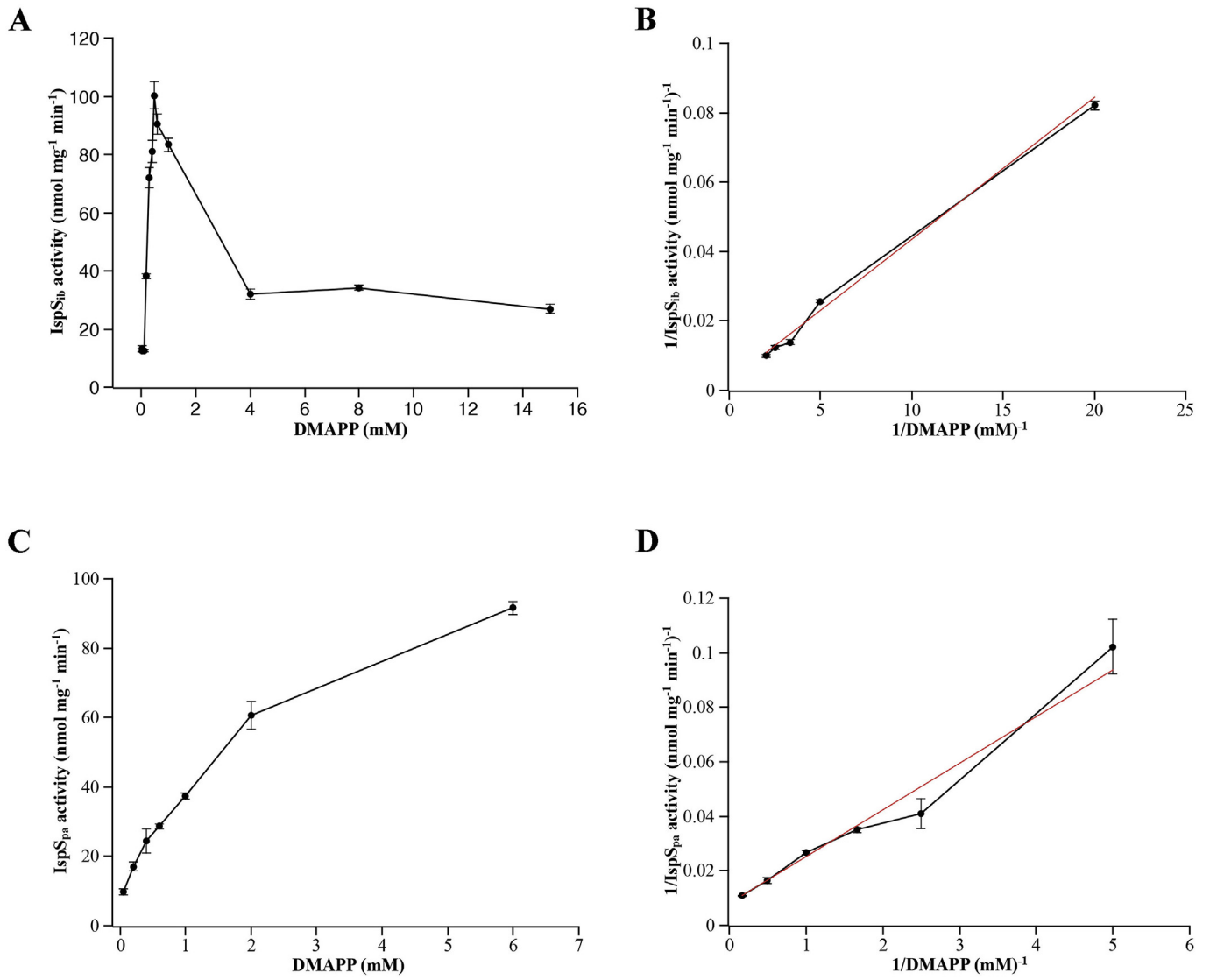

FIG. 6. DMAPP dependence of $IspS_{ib}$ and $IspS_{pa}$. (A) $IspS_{ib}$ activity was measured in 50 mM HEPES buffer (pH 7.8) containing 50 mM KCl, 50 mM $MgCl_2$, 5 μL of glycerol, 5 mM DTT, 1 μg of purified enzyme, and DMAPP (0–15 mM) at 37°C for 10 min. (B) Lineweaver–Burk plot analysis was conducted to estimate the K_m (0.2 mM) and k_{cat} (0.37 s^{-1}) of $IspS_{ib}$. (C) $IspS_{pa}$ activity was measured in the reactions mentioned above. (D) Lineweaver–Burk plot analysis was conducted to estimate the K_m (0.34 mM) and k_{cat} (0.15 s^{-1}) of $IspS_{pa}$. Values are reported as mean ± SD of triplicate experiments.

K_m ratio of $IspS_{pa}$ was determined to be 0.44. Actually, the K_m and k_{cat} values of $IspS_{pa}$ were measured in several studies, and different values were obtained (Table 2) (20). The differences in enzyme reaction systems may be the reason for these differences. The K_m and k_{cat} values of IspSs from other species were summarized and compared with those of $IspS_{ib}$ and $IspS_{pa}$ (Table 2). It is worth noting that the K_m of $IspS_{ib}$ was lower than those of most of the other IspSs, and that k_{cat} of $IspS_{ib}$ was higher than those of most of other IspSs. The high k_{cat}/K_m ratio of $IspS_{ib}$ indicated that $IspS_{ib}$ is a more competitive enzyme than commonly used $IspS_{pa}$. Isoprene synthase from *Eucalyptus globulus* has a K_m value similar to that of $IspS_{ib}$ and a high k_{cat} value (0.195 s^{-1}), albeit not higher than that of $IspS_{ib}$ (Table 2). Interestingly, the enzyme activity decreased when the DMAPP concentration was high, which has also been observed with the IspSs with low K_m values: 0.6 mM for $IspS_{ib}$, 0.9 mM for $IspS_{eg}$, and 2 mM for IspS from *C. introflexus* (23,28). Accordingly, for IspSs with high K_m values, higher DMAPP concentration, 10 mM for IspSs from tropical trees, and 5 mM for IspS from *Populus* × *canescens* was demonstrated to inhibit enzyme activity (13,20).

In a previous study, more isoprene was produced when $IspS_{pa}$ overexpressed in the engineered strain was replaced by $IspS_{ib}$ (unpublished data). The biochemical properties of $IspS_{ib}$, as a promising enzyme used for engineered strain, were analyzed in this study. The pH dependence and temperature dependence of $IspS_{ib}$ activity were analyzed and bell-shaped curves were obtained. The optimum pH of $IspS_{ib}$ was 8.6 and the optimum temperature was 42°C. Metal ion dependence of $IspS_{ib}$ activity was also performed. Mg^{2+} with an optimum 56 mM concentration was needed for enzyme activation. Then, DMAPP dependence of $IspS_{ib}$ activity was performed and Michaelis–Menten constant was measured. $IspS_{ib}$ showed higher k_{cat}/K_m ratio than the widely used $IspS_{pa}$, which indicates that $IspS_{ib}$ is a competitive candidate for the bio-isoprene production. However, stability assay indicated that $IspS_{ib}$ was an extremely thermal unstable enzyme. Enzyme engineering effort, such as direction evolution or semi-rational evolution, is required

for further research. Analysis of enzyme structure stability, such as B-factor analysis, may guide further enzyme optimization.

ACKNOWLEDGMENTS

This work was supported by National Natural Science Foundation of China (NSF No. 31400084), Hainan's Key Project of Research and Development Plan (No. ZDYF2017155), Taishan Scholars Climbing Program of Shandong (No. TSPD20150210), Youth Innovation Promotion Association CAS (No. 2017252).

References

1. **Sharkey, T. D., Wiberley, A. E., and Donohue, A. R.:** Isoprene emission from plants: why and how, Ann. Bot., **101**, 5–18 (2008).
2. **Tattini, M., Velikova, V., Vickers, C., Brunetti, C., Ferdinando, D. M., Trivellini, A., Fineschi, S., Agati, G., Ferrini, F., and Loreto, F.:** Isoprene production in transgenic tobacco alters isoprenoid, non-structural carbohydrate and phenylpropanoid metabolism, and protects photosynthesis from drought stress, Plant Cell Environ., **37**, 1950–1964 (2014).
3. **Laothawornkitkul, J., Paul, N. D., Vickers, C. E., Possell, M., Taylor, J. E., Mullineaux, P. M., and Hewitt, C. N.:** Isoprene emissions influence herbivore feeding decisions, Plant Cell Environ., **31**, 1410–1415 (2008).
4. **Ruzicka, L.:** The isoprene rule and the biogenesis of terpenic compounds, Experientia, **9**, 357–367 (1953).
5. **Claeys, M., Graham, B., Vas, G., Wang, W., Vermeylen, R., Pashynska, V., Cafmeyer, J., Guyon, P., Andreae, M. O., Artaxo, P., and Maenhaut, W.:** Formation of secondary organic aerosols through photooxidation of isoprene, Science, **303**, 1173–1176 (2004).
6. **Kim, J. H., Wang, C., Jang, H. J., Cha, M. S., Park, J. E., Jo, S. Y., Choi, E. S., and Kim, S. W.:** Isoprene production by *Escherichia coli* through the exogenous mevalonate pathway with reduced formation of fermentation byproducts, Microb. Cell Fact., **15**, 214 (2016).
7. **Lichtenthaler, H. K.:** The 1-deoxy-d-xylulose-5-phosphate pathway of isoprenoid biosynthesis in plants, Annu. Rev. Plant Physiol. Plant Mol. Biol., **50**, 47–65 (1999).
8. **Rasulov, B., Hüve, K., Bichele, I., Laisk, A., and Niinemets, Ü.:** Temperature response of isoprene emission *In vivo* reflects a combined effect of substrate limitations and isoprene synthase activity: a kinetic analysis, Plant Physiol., **154**, 1558–1570 (2010).
9. **Wiberley, A. E., Donohue, A. R., Westphal, M. M., and Sharkey, T. D.:** Regulation of isoprene emission from poplar leaves throughout a day, Plant Cell Environ., **32**, 939–947 (2009).
10. **Mayrhofer, S., Teuber, M., Zimmer, I., Louis, S., Fischbach, R. J., and Schnitzler, J. P.:** Diurnal and seasonal variation of isoprene biosynthesis-related genes in grey poplar leaves, Plant Physiol., **139**, 474–484 (2005).
11. **Sivy, T., Shirk, M., and Fall, R.:** Isoprene synthase activity parallels fluctuations of isoprene release during growth of *Bacillus subtilis*, Biochem. Biophys. Res. Commun., **294**, 71–75 (2002).
12. **Sharkey, T. D., Yeh, S., Wiberley, A. E., Falbel, T. G., Gong, D., and Fernandez, D. E.:** Evolution of the isoprene biosynthetic pathway in kudzu, Plant Physiol., **137**, 700–712 (2005).
13. **Schnitzler, J. P., Zimmer, I., Bachl, A., Arend, M., Fromm, J., and Fischbach, R. J.:** Biochemical properties of isoprene synthase in poplar (*Populus* × *canescens*), Planta, **222**, 777–786 (2005).
14. **Sasaki, K., Ohara, K., and Yazaki, K.:** Gene expression and characterization of isoprene synthase from *Populus alba*, FEBS Lett., **579**, 2514–2518 (2005).
15. **Fischbach, R. J., Zimmer, I., Steinbrecher, R., Pfichner, A., and Schnitzler, J. P.:** Monoterpene synthase activities in leaves of *Picea abie* (L.) Karst. and *Quercus ilex* L, Phytochemistry, **54**, 257–265 (2000).
16. **Ilmen, M., Oja, M., Huuskonen, A., Lee, S., Ruohonen, L., and Jung, S.:** Identification of novel isoprene synthases through genome mining and expression in *Escherichia coli*, Metab. Eng., **31**, 153–162 (2015).
17. **Koksal, M., Zimmer, I., Schnitzler, J. P., and Christianson, D. W.:** Structure of isoprene synthase illuminates the chemical mechanism of teragram atmospheric carbon emission, J. Mol. Biol., **402**, 363–373 (2010).
18. **Zurbriggen, A., Kirst, H., and Melis, A.:** Isoprene production via the mevalonic acid pathway in *Escherichia coli* (bacteria), Bioenergy Res., **5**, 814–828 (2012).
19. **Yang, J., Zhao, G., Sun, Y., Zheng, Y., Jiang, X., Liu, W., and Xian, M.:** Bio-isoprene production using exogenous MVA pathway and isoprene synthase in *Escherichia coli*, Bioresour. Technol., **104**, 642–647 (2012).
20. **Oku, H., Inafuku, M., Ishikawa, T., Takamine, T., Ishmael, M., and Fukuta, M.:** Molecular cloning and biochemical characterization of isoprene synthases from the tropical trees *Ficus virgata, Ficus septica*, and *Casuarina equisetifolia*, J. Plant Res., **128**, 849–861 (2015).
21. **Gao, X., Gao, F., Liu, D., Zhang, H., Nie, X., and Yang, C.:** Engineering the methylerythritol phosphate pathway in cyanobacteria for photosynthetic isoprene production from CO_2, Energy Environ. Sci., **9**, 1400–1411 (2016).
22. **Yang, J., Xian, M., Su, S., Zhao, G., Nie, Q., Jiang, X., Zheng, Y., and Liu, W.:** Enhancing production of bio-isoprene using hybrid MVA pathway and isoprene synthase in *E. coli*, PLoS One, **7**, e33509 (2012).
23. **Lantz, A. T., Cardiello, J. F., Gee, T. A., Richards, M. G., Rosenstiel, T. N., and Fisher, A. J.:** Biochemical characterization of an isoprene synthase from *Campylopus introflexus* (heath star moss), Plant Physiol. Biochem., **94**, 209–215 (2015).
24. **Schnitzler, J. P., Arenz, R., Steinbrecher, R., and Lehning, A.:** Characterization of an isoprene synthase from leaves of *Quercus petraea* (Mattuschka) Liebl, Bot. Acta, **109**, 216–221 (1996).
25. **Lehning, A., Zimmer, I., Steinbrecher, R., Bruggemann, N., and Schnitzler, J. P.:** Isoprene synthase activity and its relation to isoprene emission in *Quercus robur* L. leaves, Plant Cell Environ., **22**, 495–504 (1999).
26. **Monson, R. K., Jaeger, C. H., Adams, W. W., Driggers, E. M., Silver, G. M., and Fall, R.:** Relationships among isoprene emission rate, photosynthesis, and isoprene synthase activity as influenced by temperature, Plant Physiol., **98**, 1175–1180 (1992).
27. **Loivamaki, M., Louis, S., Cinege, G., Zimmer, I., Fischbach, R. J., and Schnitzler, J. P.:** Circadian rhythms of isoprene biosynthesis in grey poplar leaves, Plant Physiol., **143**, 540–551 (2007).
28. **Sharkey, T. D., Gray, D. W., Pell, H. K., Breneman, S. R., and Topper, L.:** Isoprene synthase genes form a monophyletic clade of acyclic terpene synthases in the Tps-B terpene synthase family, Evolution, **67**, 1026–1040 (2013).
29. **Silver, G. M. and Fall, R.:** Characterization of aspen isoprene synthase, an enzyme responsible for leaf Isoprene emission to the atmosphere, J. Biol. Chem., **270**, 13010–13016 (1995).
30. **Silver, G. M. and Fall, R.:** Enzymatic synthesis of isoprene from dimethylallyl diphosphate in aspen leaf extracts, Plant Physiol., **97**, 1588–1591 (1991).
31. **Wildermuth, M. C. and Fall, R.:** Light-dependent isoprene emission: characterization of a thylakoid-bound isoprene synthase in *Salix discolor* chloroplasts, Plant Physiol., **112**, 171–182 (1996).
32. **Wildermuth, M. C. and Fall, R.:** Biochemical characterization of stromal and thylakoid-bound isoforms of isoprene synthase in willow leaves, Plant Physiol., **116**, 1111–1123 (1998).
33. **Kuzma, J. and Fall, R.:** Leaf isoprene emission rate is dependent on leaf development and the level of isoprene synthase, Plant Physiol., **101**, 435–440 (1993).